

History effects in polycrystalline BCC metals and steel subjected to rapid changes in strain rate and temperature

J. KLEPACZKO (WARSAWA) and J. DUFFY (PROVIDENCE)

A REVIEW is presented of the available experimental data on strain rate and temperature history effects for polycrystalline BCC metals and ferritic steels together with new experimental results on AISI 1020 hot rolled steel (HRS). The early experiments on steels and other BCC metals are discussed in which interrupted tests were performed at two substantially different strain rates or temperatures. These experiments revealed that a substantial difference in response exists between BCC and FCC polycrystalline metals. The review also includes results of incremental strain rate tests with large jumps in strain rate augmented by a series of experiments designed to determine strain rate history effects in steel. A literature survey on incremental tests for BCC metals and steel is also included. Experimental results for ferritic steels discussed in the paper indicate that for low temperatures as well as for the dynamic ageing temperature region strain rate history effects are shown to be of considerable importance.

Przedstawiono przegląd osiągalnych danych doświadczalnych dotyczących efektów historii prędkości odkształcenia i temperatury dla polikrystalicznych metali o sieci regularnej przestrzennie centrowanej i dla stali ferrytycznych, jak również nowe dane eksperymentalne dotyczące stali AISI 1020 walcowanej na gorąco. Przedyskutowano wcześniejsze doświadczenia ze stałą i innymi metalami typu BCC, w których wykonywane były testy przerywane przy dwóch całkowicie różnych prędkościach odkształcenia lub temperaturach. Wykazywały one istotną różnicę w zachowaniu się metali polikrystalicznych o sieci centrowanej przestrzennie i powierzchniowo. Przegląd zawiera również dane z eksperymentów z ciągłą zmianą prędkości odkształcenia i dużymi skokami tej prędkości, uzupełnione serią badań mających na celu określenie wpływu historii prędkości odkształcenia w stali i odpowiednim przeglądem literatury. Przedstawione wyniki dotyczące stali ferrytycznych wskazują, że przy niskich temperaturach i w obszarze temperatur dynamicznego starzenia efekty historii prędkości odkształcenia są znaczne.

Представлено обзрение доступных экспериментальных данных, касающихся эффектов истории скорости деформации и температуры для поликристаллических металлов с регулярной пространственно центрированной решеткой и для ферритных сталей, как тоже новые экспериментальные данные, касающиеся горячекатаной стали AISI 1020. Обсуждены более ранние эксперименты со сталью и с другими металлами типа BCC, в которых проводились тесты прекращенные при двух полностью разных скоростях деформации или температурах. Показывали они существенную разницу в поведении поликристаллических металлов с центрированными пространственно и поверхностно решетками. Обзрение содержит тоже данные из экспериментов с непрерывным изменением скорости деформации и большими скачками этой скорости, пополненные серией исследований имеющих целью определить влияние истории скорости деформации в стали и соответствующим обзрением литературы. Представленные результаты, касающиеся ферритных сталей, показывают, что при низких температурах и в области температур динамического старения, эффекты истории скорости деформации значительны.

1. Introduction

THE FLOW stress of polycrystalline metals and alloys as well as single crystals is influenced both by the temperature at which deformation occurs and by strain rate [1-4]. These effects have been extensively studied during the past decades. But only recently has it

been recognized that the strain rate and temperature deformation histories play a very important role in the plastic behavior of metals and alloys. It has been shown during the past decade that strain rate and temperature history effects are substantial in the case of polycrystals as well as monocrystals for FCC metals [5–8]. A review of available experimental data on strain rate and temperature history effects for several FCC metals was presented in [9]. However, there has been no extensive and systematic investigation and evidence of strain rate history effects for BCC metals, including steels. The main purpose of the present paper is to present a review of available experimental data in which evidence is provided of such effects. The first part of the paper is devoted to reviewing and discussing a few early experiments on steels in which interrupted tests were performed at two substantially different strain rates, i.e. plastic deformation at an initial rate, unloading and then reloading at different rate. These early experiments revealed quite a different behavior in steels than was observed in aluminum, copper and other FCC metals with regard to strain rate history effects.

The development of the torsional split Hopkinson bar made possible incremental tests without specimen unloading and with large jumps in strain rate at different initial values of strain [10]. This type of test, used initially to study FCC metals, has been applied recently to study strain rate history effects in steels. Some new results on steels are discussed in the second part of the paper.

Many investigators have observed that the flow stress of steels, including ferritic steels, is a highly nonlinear function of strain rate and temperature [11–21]. In addition, tests on some BCC metals also show a highly complicated plastic response with regard to strain rate and temperature [22]. However, the majority of these results, or at least those obtained at high strain rates, were obtained for the case where temperature is held fixed and a single strain rate is imposed during each test. While the results are of great value, they do not fully reflect the complications inherent in metal and alloy behavior of BCC structure. Minima and maxima of the flow stress which are observed at different ranges of temperatures and strain rates, usually associated with diffusion controlled dislocation processes may cause both temperature history effects and strain rate history effects within an intermediate temperature range (0.3 to 0.5 of melting temperature). In addition, dynamic strain ageing effects associated with diffusion processes may produce the appearance of a negative strain rate sensitivity if experiments are limited to different constant strain rates. As will be shown later, the full complexity of strain rate history effects in BCC metals is only brought out by experiments in which the imposed strain rate is not constant and, in particular, by experiments in which substantial jumps in strain rate are imposed.

2. Results of early interrupted experiments

One of the most useful experiments developed thus far to obtain satisfactory information on dynamic plastic deformation of metals involves the imposition during the course of deformation of a sudden increment in strain rate or a sudden change in temperature. Many of the investigations of rate effects at low strain rates have been carried out by making small sudden changes of the deformation rate during the test, see for example

[23]. But a convincing demonstration of deformation history effects by means of a rapid change in strain rate frequently requires an increment of more than three orders of magnitude. Because of technical difficulties in developing the incremental experiment, the first attempts to investigate strain rate or temperature history involved interrupted testing in which the specimen was completely unloaded before the new strain rate or temperature was imposed. Thus, in interrupted tests specimens are loaded into the plastic range at one strain rate or temperature, unloaded, and then reloaded at a substantially different strain rate or temperature. The flow stresses are then compared with those obtained in test conducted at entirely constant strain rates or temperatures.

In the earliest experiments with steels and other BCC metals rapid changes in temperature with partial specimen unloading rather than strain rate changes were imposed [24, 25]. Later the results of temperature-change experiments were reported for mild steel in [26] where prestraining was imposed at room temperature and further straining was continued at much lower temperatures. Those early experiments indicated that for polycrystalline BCC metals, tested at relatively low and ambient temperatures, temperature history effects do not dominate at small strains, up to $\epsilon \approx 0.10$.

The interrupted strain rate experiments [27, 28] demonstrated that after repeated compression impact of medium-carbon steel at room temperature, the reloading portion of the quasi-static stress-strain curve is lower than the curve obtained entirely at the quasi-static strain rate. The results obtained in [27] for medium-carbon steel (0.32% C; 0.62% Mn; 0.23% Si) are shown in Fig. 1, the numbers on the dynamic curves denote

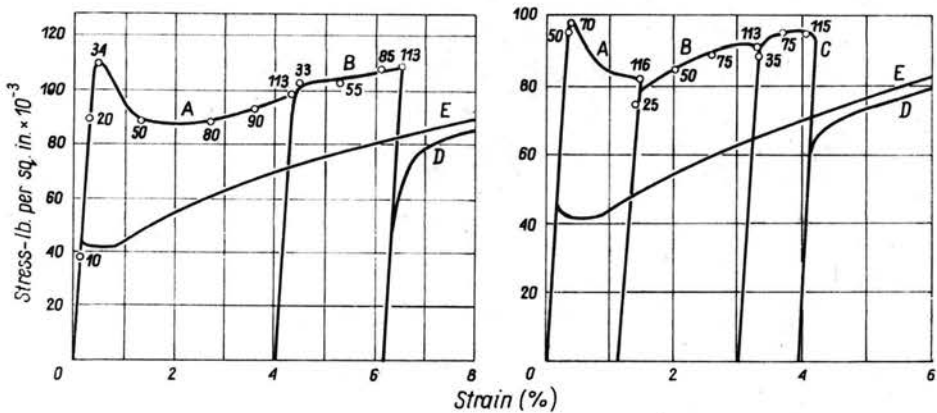


FIG. 1. Repeated impact tests on medium carbon steel 0.32% C; upper part: dynamic curves $A - \dot{\epsilon} \approx 3.5 \times 10^2 \text{ s}^{-1}$, $B - \dot{\epsilon} \approx 2 \times 10^2 \text{ s}^{-1}$, D and E quasi-static curves, $\dot{\epsilon} \approx 10^{-3} \text{ s}^{-1}$; lower part: dynamic curves $A - \dot{\epsilon} \approx 10^2 \text{ s}^{-1}$, $B - \dot{\epsilon} \approx 1.6 \times 10^2 \text{ s}^{-1}$, $C - \dot{\epsilon} \approx 78 \text{ s}^{-1}$, D and E quasi-static curves, $\dot{\epsilon} \approx 10^{-3} \text{ s}^{-1}$; curves D for both parts obtained after dynamic prestraining; numbers denote time in microseconds; after [27], (note: 1 lb. per sq. in. $\times 10^3 = 6.895 \text{ MPa}$).

the time in microseconds. In Fig. 1 the dynamic stress-strain curves are denoted by A , B and C , the entirely quasi-static curves are E ; whereas curves D were obtained during slow deformation after dynamic straining. Similar results were obtained for the same steel in [28], see Fig. 2. In this case only the quasi-static curves are reproduced. These curves were obtained immediately after impact loading and it is seen that for curves A ,

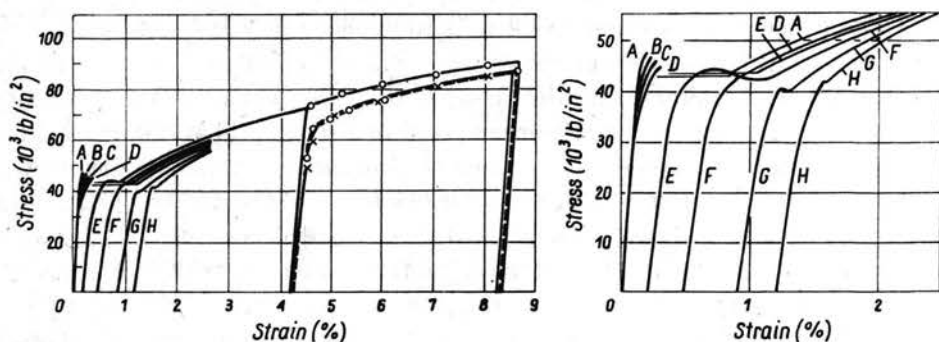


FIG. 2. Repeated impact tests on medium carbon steel 0.32% C; *A, B and C* quasi-static curves after pulsing without yielding; *D, E, F and H* quasi-static curves after small dynamic straining; — quasi-static curve after prior slow straining to $\epsilon_t = 0.042$, *x* — quasi-static curve after dynamic straining $\epsilon_t = 0.042$ at $T = 288$ K and $\dot{\epsilon}_t \approx 1.6 \times 10^3$ s⁻¹, — quasi-static curve after dynamic straining $\epsilon_t = 0.042$ at $T = 189$ K and $\dot{\epsilon}_t \approx 8.9 \times 10^2$ s⁻¹; after [28], (note: 1 lb. per sq. in. $\times 10^3 = 6.895$ MPa).

B, C and D the static upper yield stress is indeed reduced by pulsing without yielding. In the case of small dynamic prestrains, curves *E, F, G and H*, the lower yield stress and the flow stress is gradually reduced after impact loading. It is also to be observed that an upper yield point persists in a reduced form even after dynamic straining of ~ 0.01 , curves *G and H*. Also the quasi-static portions of the stress-strain curves were obtained after prior dynamic straining up to 0.042 at two temperatures, $T = 189$ K and $T = 288$ K (room temperature), see the upper part of Fig. 2. It is again observed that in the interrupted strain rate test the flow stress resulting from quasi-static reloading is reduced by about 10 percent in the case of dynamic prestraining, but is unaffected in the case of quasi-

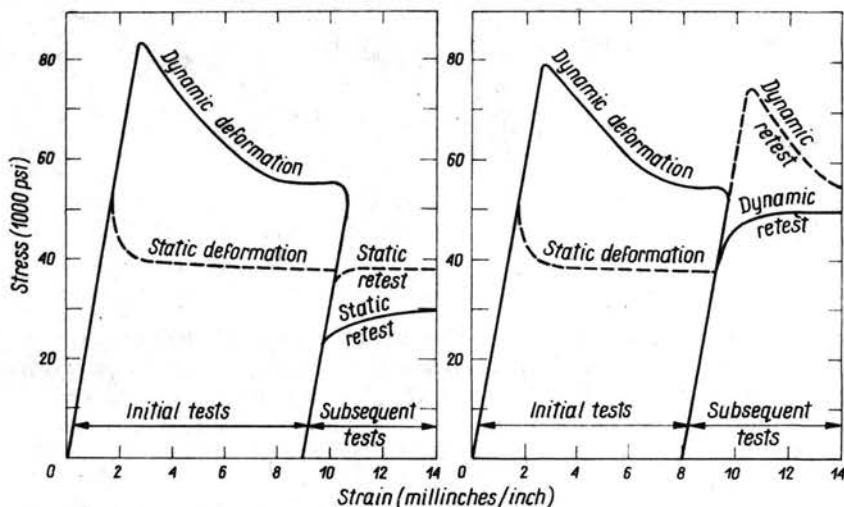


FIG. 3. Interrupted strain rate experiments on low-carbon steel, SAE 1010 plate (0.1% C); upper part: dotted line — quasi-static deformation at 2.2×10^{-7} s⁻¹, solid line — dynamic deformation up to $\epsilon_t = 0.009$ at $\dot{\epsilon}_t \approx 7.5$ s⁻¹ and subsequent quasi-static straining at $\dot{\epsilon}_t = 2.2 \times 10^{-7}$ s⁻¹; lower part: solid line — dynamic deformation at $\dot{\epsilon}_t \approx 7.5$ s⁻¹, dotted line quasi-static deformation up to $\epsilon_t = 0.008$ at $\dot{\epsilon}_t = 2.2 \times 10^{-7}$ s⁻¹ and subsequent dynamic deformation at $\dot{\epsilon}_t \approx 7.5$ s⁻¹, after [29], (note: 1×10^3 psi = 6.985 MPa).

-static prestraining. These results clearly demonstrate the existence of strain rate history effects for medium-carbon steel. Metallographic examination of this steel showed that during loading at an average initial strain rate of $2 \times 10^2 \text{ s}^{-1} \leq \dot{\epsilon} \leq 3.5 \times 10^2 \text{ s}^{-1}$ (Fig. 1) plastic deformation occurs by fine slip, but during slower straining at $\dot{\epsilon} \approx 10^{-3} \text{ s}^{-1}$ the slip bands are coarser.

Results of interrupted strain rate experiments on SAE 1010 low carbon steel (0.1% C; 0.3% Mn; 0.16% Si) were reported in [29], and they are shown in Fig. 3. In the upper part of Fig. 3 the quasi-static tensile stress-strain curves are shown after both initial quasi-static and initial dynamic deformation to a plastic strain $\epsilon_t = 0.009$. It was demonstrated again that the quasi-static portion of the stress-strain curve after initial dynamic tensile deformation and subsequent unloading is lower by about 28% than the entirely quasi-static curve obtained with the same unloading procedure (see solid curve in the upper portion of Fig. 3). In addition, in the lower portion of Fig. 3, curves are shown which are obtained on reloading dynamically after initial quasi-static or dynamic deformation up to $\epsilon_t = 0.008$ and subsequent unloading. Here the inverse situation is observed, dynamic tensile loading after initial quasi-static deformation leads to substantially higher flow stress compared to the dynamic reloading curve after initial dynamic deformation (see dotted curve). Another important feature of these results is the sharp yield point that occurs as a result of dynamic reloading after quasi-static deformation (see dynamic retest-dotted curve). Dynamic and quasi-static strain rates applied in [29] were respectively $\dot{\epsilon} = 7.5 \text{ s}^{-1}$ and $\dot{\epsilon} = 2.2 \times 10^{-7} \text{ s}^{-1}$. In the case of dynamic loading the load-time function was approximately that of a half-period sine wave lasting almost 1 ms. Consequently the strain rate was not constant during the test and once again a complicated strain rate history effect was revealed for steel.

The complicated nature of strain rate history effects for high purity iron was demonstrated by HARDING [30], who performed interrupted tests with annealed specimens loaded in tension, Fig. 4. Curve *A* was obtained by loading at the strain rate of 10^3 s^{-1} after

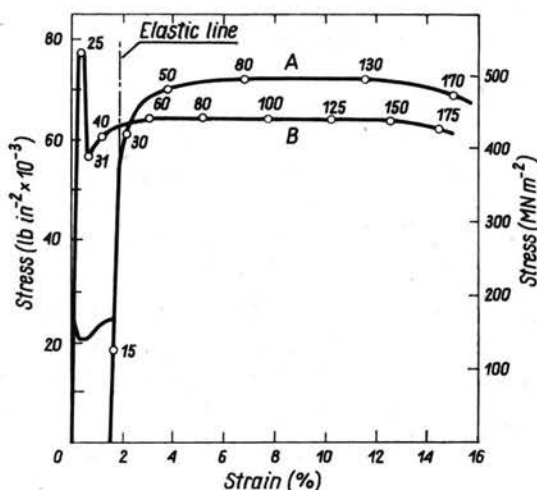


FIG. 4. Stress-strain curves for high purity annealed iron; *A*—interrupted test, *B*—constant strain rate test. Numbers indicate times of deformation in μs , after [30], courtesy of The Institute of Physics.

imposing a small prestrain ($\epsilon_i = 0.016$) at the quasi-static rate of 10^{-3} s^{-1} . The result is compared to curve *B* obtained at a continuous strain rate of $\sim 10^3 \text{ s}^{-1}$. This result is to some extent similar to that of Smith (Fig. 3), however, during dynamic reloading the upper yield point is not observed. The fact that for both cases a higher dynamic flow stress is found in the interrupted tests contrasts with the behavior of FCC metals in which prestrain at the lower strain rate reduces the subsequent flow stress at the higher rate [9].

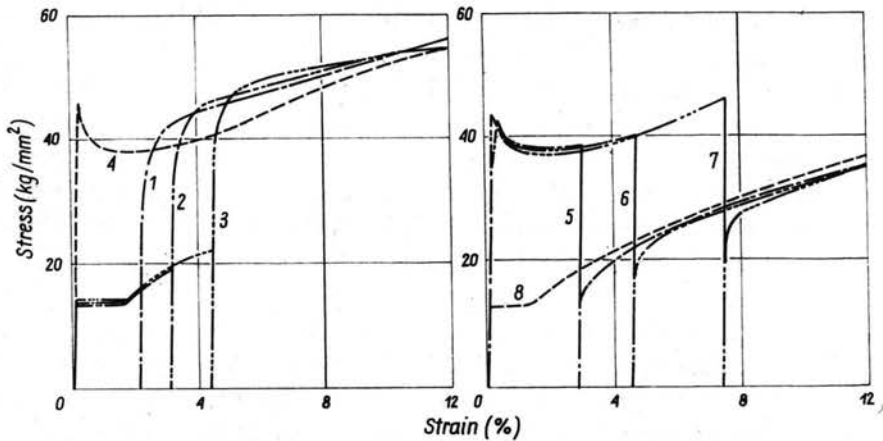


FIG. 5. The effect of quasi-static prestrain at $\dot{\epsilon} \approx 1.2 \times 10^{-3} \text{ s}^{-1}$ on the subsequent dynamic deformation of low carbon steel 0.03% C at $\dot{\epsilon} = 4 \times 10^2 \text{ s}^{-1}$ (top); and the effect of dynamic prestrain at $\dot{\epsilon} \approx 4 \times 10^2 \text{ s}^{-1}$ on subsequent quasi-static deformation at $\dot{\epsilon} = 1.2 \times 10^{-3} \text{ s}^{-1}$ (bottom); after [45].

The same behavior was observed for low carbon steel (0.02% C) in [45], as shown in Fig. 5. In those interrupted experiments the split Hopkinson pressure bar was used along with a standard testing machine.

3. Results of early incremental experiments

As mentioned above, the incremental strain rate experiment is probably the most useful one for studying history effects. The earliest incremental results involving high strain rates reported for steel are those of NICHOLAS [31]. Tubular specimens of an AISI 1020 steel were tested in torsion using a pneumatically driven piston acting through a lever arm to apply a dynamic torque; at the other end of the specimen a motor was used to apply a torque quasi-statically. The maximum shear strain rate attained in these experiments was $\dot{\gamma} = 25 \text{ s}^{-1}$. Nicholas' results for the dynamic strain rate $\dot{\gamma}_r = 25 \text{ s}^{-1}$ preceded by a static shear prestrain of $\gamma_i = 0.02$ are shown in Fig. 6, and they are consistent with those of SMITH [29] HARDING [30] and TANAKA [45]. The upper part of Fig. 6 shows the stress-strain diagrams for constant shear strain rates, $10^{-3} \text{ s}^{-1} \leq \dot{\gamma} \leq 25 \text{ s}^{-1}$, the lower part presents the results of the incremental test. It is apparent that with incremental loading the resulting flow stress is generally higher than in a constant-rate dynamic test. Thus the results of the incremental test is again consistent with the previously discussed results of interrupted tests. Thus all of these results for steels show that the flow stress after

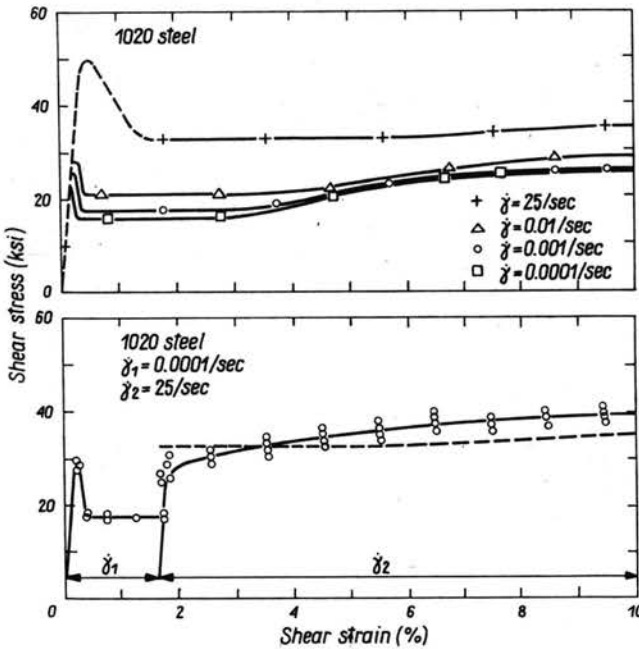


FIG. 6. Results of incremental tests for AISI 1020 steel, the dashed line represents a constant strain rate test of $\sim 25 \text{ s}^{-1}$, after [31].

a strain rate increment is higher than would result from deforming only at the dynamic strain rate.

On the other hand strain rate history effects are not always observed in steels. For example, incremental stress wave propagation experiments performed on deep-drawing steel [32], revealed that at low initial tensile strains of the order of 0.01 the rate sensitivity is high although the strain rate history effect at room temperature is negligible. These results should be recognized as preliminary since the incremental portion of the stress-strain diagram was obtained by an integration of the wave equation. The initial values of strain were $\varepsilon_i \approx 3.6 \times 10^{-3}$ and 7×10^{-3} and the initial strain rate $\dot{\varepsilon}_i \approx 10^{-3} \text{ s}^{-1}$, the average dynamic strain rate was $\dot{\varepsilon}_r \approx 1.4 \times 10^2 \text{ s}^{-1}$.

An experimental study of room temperature rate sensitivity of AISI type 304 stainless steel subjected to cyclic loading in the strain rate region of $10^{-5} \text{ s}^{-1} \leq \dot{\varepsilon} \leq 10^{-3} \text{ s}^{-1}$ revealed no strain rate history effect [33].

With reference to other BCC metals, CAMPBELL [1] and BRIGGS and CAMPBELL [22] reported results of incremental tests on annealed polycrystalline molybdenum and niobium. Tests were performed in compression in either one of two machines depending on the desired strain rate region. In either case the strain rate change was from a lower to higher strain rate, and the change was imposed after an accumulation of a strain $\varepsilon_i \approx 0.08$. By means of a standard testing machine, strain rates were attained ranging from $1.7 \times 10^{-4} \text{ s}^{-1}$ to $8.3 \times 10^{-3} \text{ s}^{-1}$; a hydraulically operated machine provided strain rates from $8.5 \times 10^{-3} \text{ s}^{-1}$ to 10^2 s^{-1} . The results for molybdenum and niobium are shown respectively in Figs. 7 and 8. The incremental results were compared with those of tests conducted

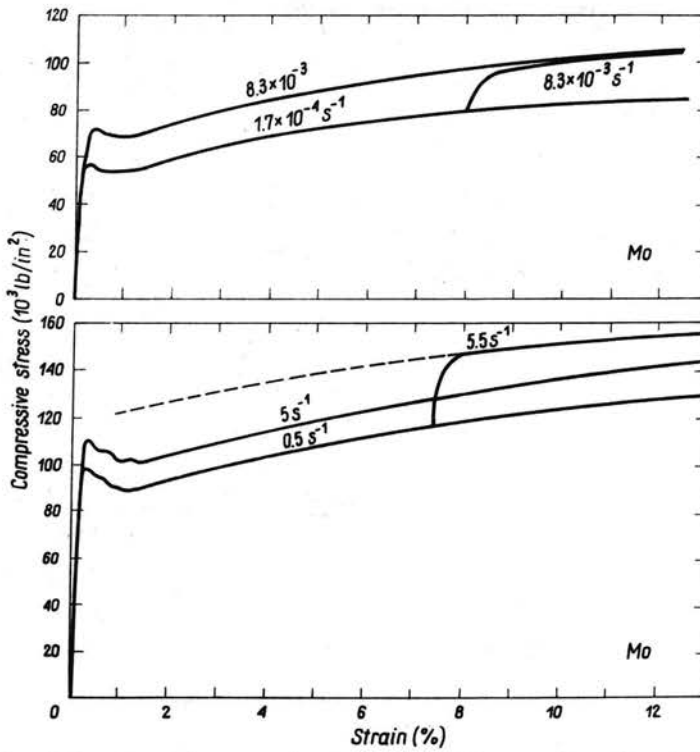


FIG. 7. Results of incremental tests for molybdenum, after [1] and [22].

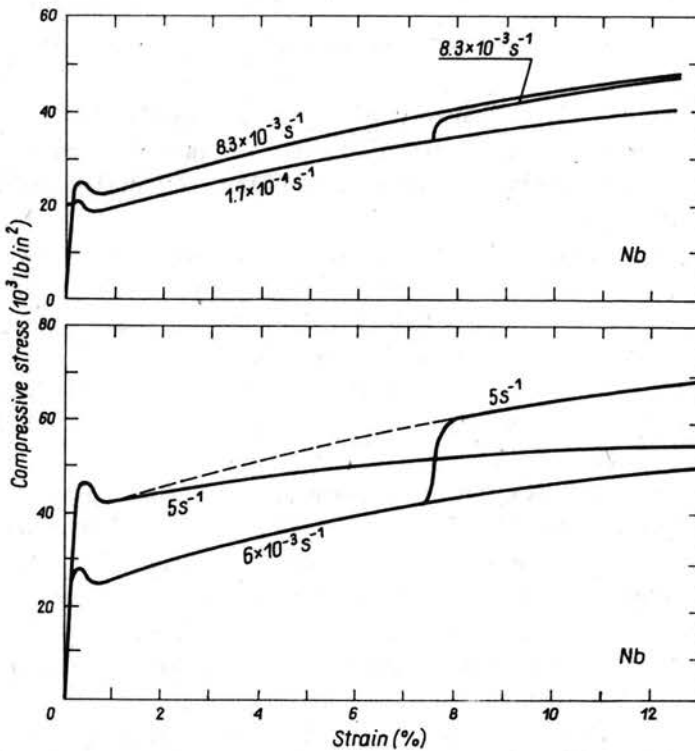


FIG. 8. Results of incremental tests for niobium, after [1] and [22].

at constant strain rates to show that the flow stress in both materials depends on strain rate history. Furthermore, as it is seen in Figs. 7 and 8, significantly different results are obtained within each of the two strain rate ranges and depending on the deformation rate history. These differences vary in a complex manner with the initial and final strain rate. For molybdenum (Fig. 7) a strain rate change from $\dot{\epsilon}_i = 0.51 \text{ s}^{-1}$ to $\dot{\epsilon}_r = 5.5 \text{ s}^{-1}$ produces a result qualitatively similar to that shown for steel (Figs. 3, 4 and 5). But in the lower strain rate region a strain rate change from $\dot{\epsilon}_i = 1.7 \times 10^{-4} \text{ s}^{-1}$ to $\dot{\epsilon}_r = 8.3 \times 10^{-3} \text{ s}^{-1}$ exhibits the opposite result: the incremental portion of the stress-strain diagram is lower than that obtained at the entirely constant strain rate $\dot{\epsilon} = 8.3 \times 10^{-3} \text{ s}^{-1}$. A similar result was obtained from incremental strain rate experiments within the same ranges of strain rate for niobium (Fig. 8).

4. Results of incremental tests with large jumps in strain rate

During the last decade considerable improvements have been achieved in the experimental techniques used to test metals under dynamic conditions. These have led to more reliable results especially in incremental type experiments in the high strain rate region. The experimental method most commonly used for this purpose is probably the split-Hopkinson bar modified for torsional loading [10, 34]. This apparatus employs a thin tubular specimen loaded in torsion and subjected to a strain rate increment typically of six orders of magnitude at relatively large strains and over a wide range of temperatures.

This technique was first successfully used to demonstrate strain rate history effects at room temperature for FCC metals, including aluminum [10], copper [7, 8, 35], and lead [36]. Incremental tests at various temperatures using the modified torsional Hopkinson bar have been reported for copper [7] and [8]. HCP metals were also tested at different temperatures using this technique: magnesium and zinc [7], titanium [8].

A systematic study of strain rate history effects using large jumps in strain rate was performed by Campbell and associates [8, 37]. The increments in strain rate were

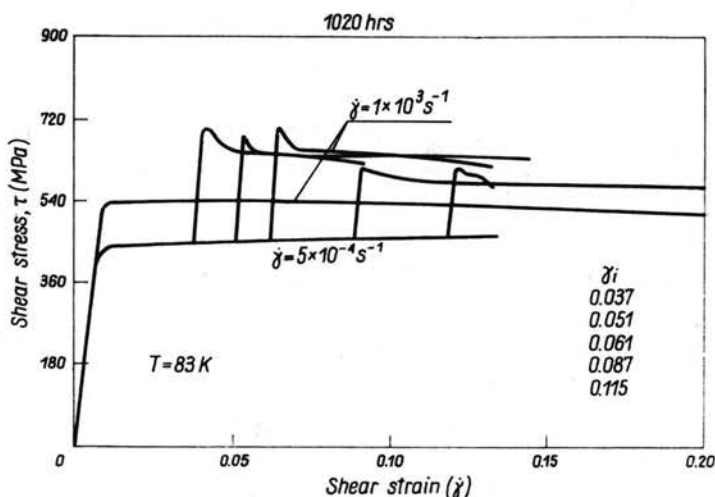


FIG. 9. Results of constant and incremental strain rate tests on AISI 1020 hot rolled steel at 83 K.

imposed at shear strains γ_i equal successively to 0.08; 0.20, and 0.34, with an initial strain rate $\dot{\gamma}_i = 6 \times 10^{-3} \text{ s}^{-1}$ and a dynamic rate $\dot{\gamma}_r = 1.2 \times 10^3 \text{ s}^{-1}$. Specimens were tested at six nominal temperatures ranging from 123 K to 673 K.

The same experimental technique was used by WILSON *et al.* [38] to perform incremental strain rate tests at room temperature on two low carbon steels, AISI 1020 hot rolled and AISI 1018 cold rolled steel. The purpose of the investigation was to determine the influence of strain rate and strain rate history on steels of nearly identical composition but of quite different forming histories. Strain rate history effects in both steels, as measured at the ambient temperature, appear to be small in this case.

These results show that the effects of strain rate history in polycrystalline BCC metals are still not well known. This situation is due in large measure to the limited amount of systematic experimental data, especially over a fairly extended temperature range.

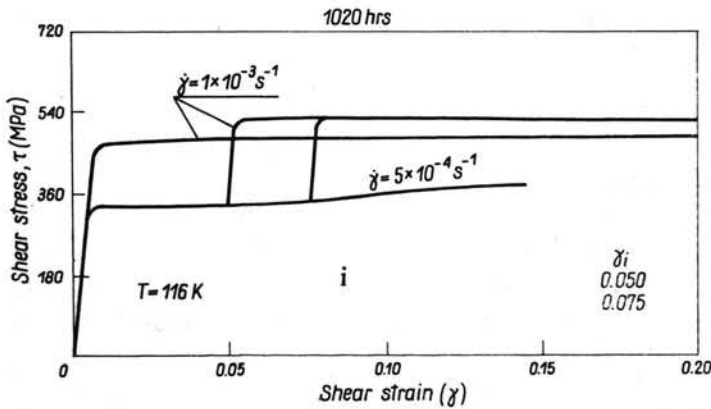


FIG. 10. Results of constant and incremental strain rate tests on AISI 1020 hot rolled steel at 116 K.

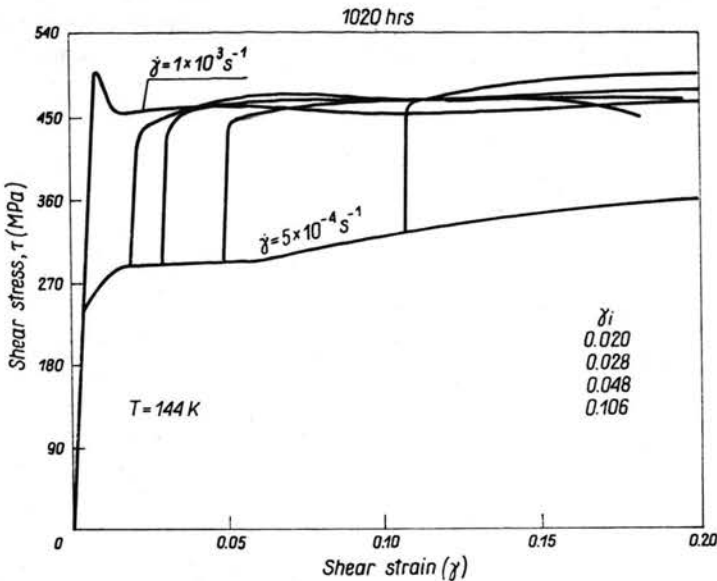


FIG. 11. Results of constant and incremental strain rate tests on AISI 1020 hot rolled steel at 144 K.

Recently a series of experiments was performed on specimens of AISI 1020 hot rolled steel (HRS), with composition 0.25% C; 0.50% Mn; 0.017% P; 0.029% S using the torsional split Hopkinson bar [39]. Stress-strain curves at a quasi-static shear strain rate $\dot{\gamma}_i \approx 5 \times 10^{-4} \text{ s}^{-1}$, a dynamic strain rate $\dot{\gamma}_r \approx 10^3 \text{ s}^{-1}$, and those resulting from incremental strain rate tests between these two strain rates were obtained at twelve temperatures ranging from 83 K to 394 K. The strain rate increments were imposed at initial shear strains γ_i , ranging from 0.02 to 0.10. Representative results for five temperatures (83 K, 116 K, 144 K, 294 K and 394 K) are shown in Figs. 9–13. As expected, and as made evident from the constant strain rate test, the strain rate has a significant effect on the flow stress of 1020 HRS at all temperatures. However, the stress-strain curves obtained in some of the incremental experiments show that the flow stress after the increment in strain rate is higher than the flow stress level obtained at the entirely constant high strain rate for the same strain. This effect is substantial at the lowest temperature tested, 83 K,

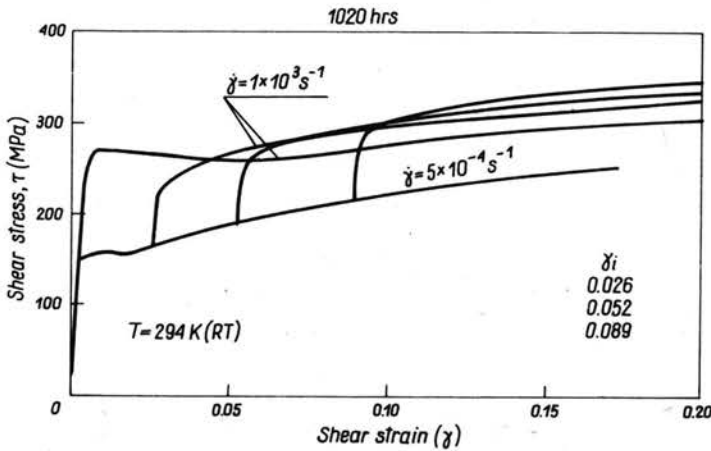


FIG. 12. Results of constant and incremental strain rate tests on AISI 1020 hot rolled steel at 294 K — RT.

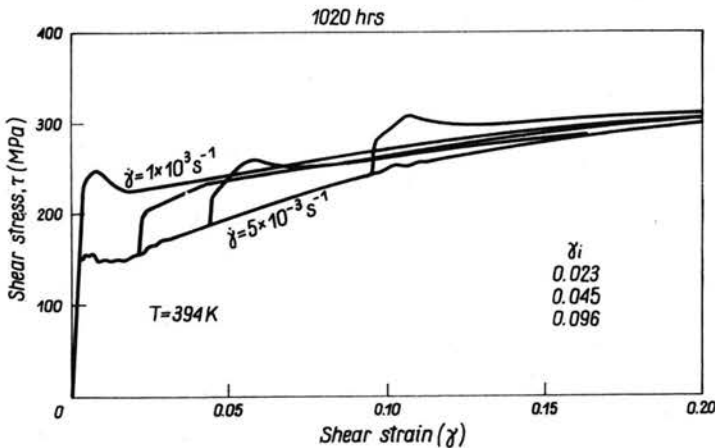


FIG. 13. Results of constant and incremental strain rate tests on AISI 1020 hot rolled steel at 394 K.

less pronounced at 116 K and is almost invisible at 144 K. But at 394 K the incremental portion of the stress-strain curves show some transients especially at the two highest initial strains, $\gamma_i \approx 0.05$ and $\gamma_i \approx 0.10$. In addition, the quasi-static and dynamic stress-strain curves obtained at constant strain rates converge at increasing strains. These results are shown in Fig. 13. It is expected that at this temperature dynamic strain ageing starts to become important.

Strain rate history effects within the dynamic strain ageing region were observed in mild steel (0.125% C; 1.15% Mn; 0.37% P) by ELBICHE and CAMPBELL [8]. Their results for 293 K, 473 K and 673 K are shown in Figs. 14–16. The room temperature results show a well-pronounced strain rate history effect at larger strains, γ_i from 0.085 to 0.345 (Fig. 14); the black points mark the beginning of yielding during incremental loading. The results for 473 K and 673 K (Figs. 15 and 16) at a low strain rate show the occurrence

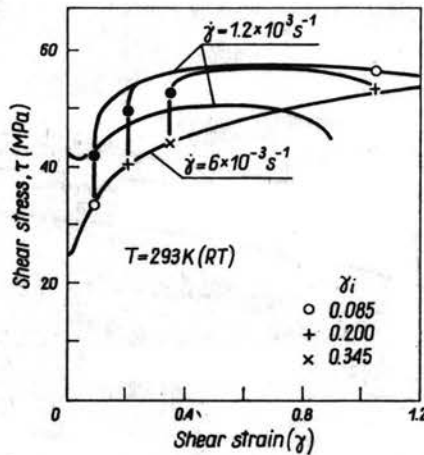


FIG. 14. Test results for mild steel (0.125% C; 1.15% Mn) at 293 K — RT, after [8].

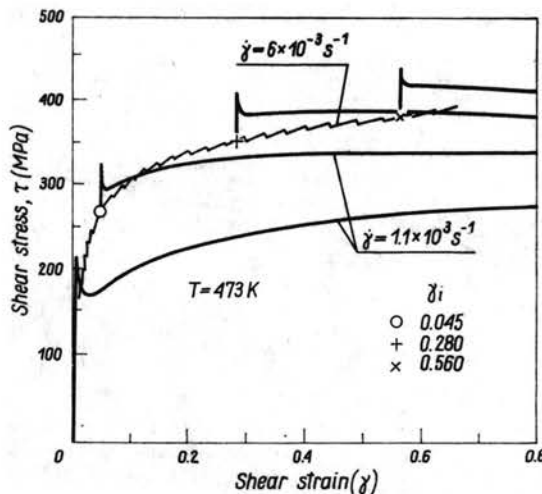


FIG. 15. Test results for mild steel (0.125% C; 1.15% Mn) at 473 K, after [8].

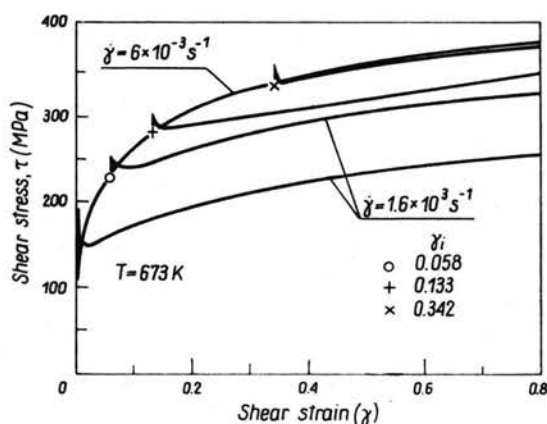


FIG. 16. Test results for mild steel (0.125% C; 1.15% Mn) at 673 K, after [8].

of dynamic strain ageing. At 473 K the stress-strain curve obtained at a strain rate of $6 \times 10^{-3} \text{ s}^{-1}$ shows serrations. Constant strain rate tests at $1.6 \times 10^3 \text{ s}^{-1}$ exhibit a negative rate sensitivity at both temperatures. For incremental experiments performed at relatively large values of γ_i a significant drop in stress was observed at the beginning of yielding. The work hardening rate in the incremental portions of the stress-strain diagrams is substantially lower than that resulting from quasi-static or dynamic deformation at constant strain rates. There is no indication of a negative strain rate sensitivity for the initial portions of the incremental tests.

Thus it appears from the above that for small values of prestrain, i.e. up to $\gamma_i \approx 0.20$, strain rate history effects for mild steel are most important in only two temperature regions: for temperatures lower than $\sim 150 \text{ K}$, and for the dynamic strain ageing temperature region ($500 \pm 100 \text{ K}$). At temperatures from 150 K to 350 K strain rate history effects for ferritic steels, although still present, are of less importance. Results are different for pre-strains greater than $\gamma_i \approx 0.20$: as pointed out by ELEICHE and CAMPBELL [8], (see Fig. 14), strain rate history effects in this range of initial strains may be substantial even at intermediate temperatures.

These experimental results obtained from both interrupted and incremental tests demonstrate the very important role of strain rate history effects in the deformation of BCC polycrystalline metals with special emphasis on low as well as on the dynamic strain ageing temperature ranges. It is also evident that substantial differences in response exist between BCC and FCC polycrystalline metals.

5. Discussion and conclusions

The experimental results presented above reveal the complicated nature of plastic yielding and flow in BCC metals. There can be no doubt that strain rate history and temperature history effects are observed not only in ferritic steels but also in polycrystalline iron, molybdenum and niobium. A more systematic study of these effects for mild steel leads to the conclusion that strain rate history effects are of great importance within the

low temperature region, $T \leq 120$ K, as well as within the strain ageing region, 350 K $\leq T \leq 750$ K. At temperatures from the ambient and down to ~ 150 K, strain rate history effects are much less pronounced. However, even at room temperature strain rate history effects were observed at strains exceeding ~ 0.15 (Fig. 14).

A comparison of strain rate history effects as measured in interrupted tests with more recent results obtained based in incremental tests seems to indicate that the unloading and reloading process is of little significance to the final result.

Incremental experiments involving a large jump in strain rate provide evidence that strain rate history effects are significantly different in polycrystalline FCC and HCP metals on the one hand and polycrystalline BCC metals on the other [5, 7, 9]. Behavior typical of BCC and FCC metals is shown in Fig. 17, although in the case of BCC metals the re-

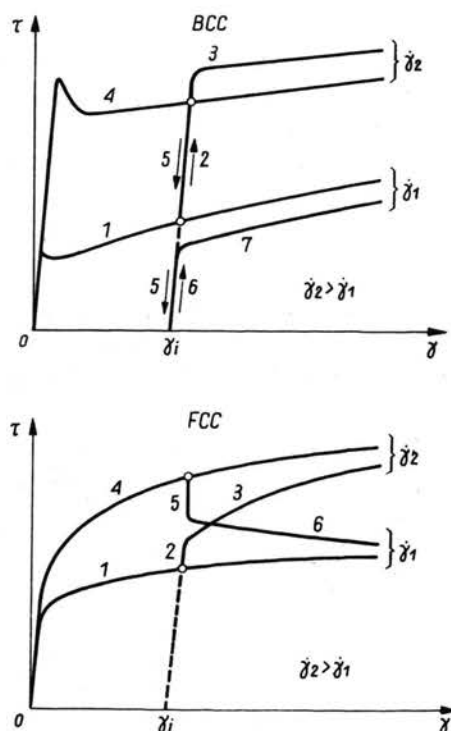


FIG. 17. Schematic representation of strain rate history effects for BCC and FCC polycrystalline metals; 1-2-3 incremental test with initial strain rate $\dot{\gamma}_i = \dot{\gamma}_1$; 4-5-6 incremental test with $\dot{\gamma}_i = \dot{\gamma}_2$, 4-5-6-7 interrupted test (BCC), γ_i —initial strain.

sults apply only to temperatures lower than the ambient. Both pictures are quite consistent, but a physical explanation of these effects in the BCC case is more complicated and will require more attention in the future. The observed behavior for BCC and FCC metals is consistent with so-called temperature history effects. Temperature history effects for FCC metals have been discussed in more detail elsewhere [9, 42]. The effect of pre-strain at room temperature on the low-temperature plastic properties of low carbon steel was reported by LINDLEY [44]. These results for 0.05% C steel are shown in Fig. 18. The

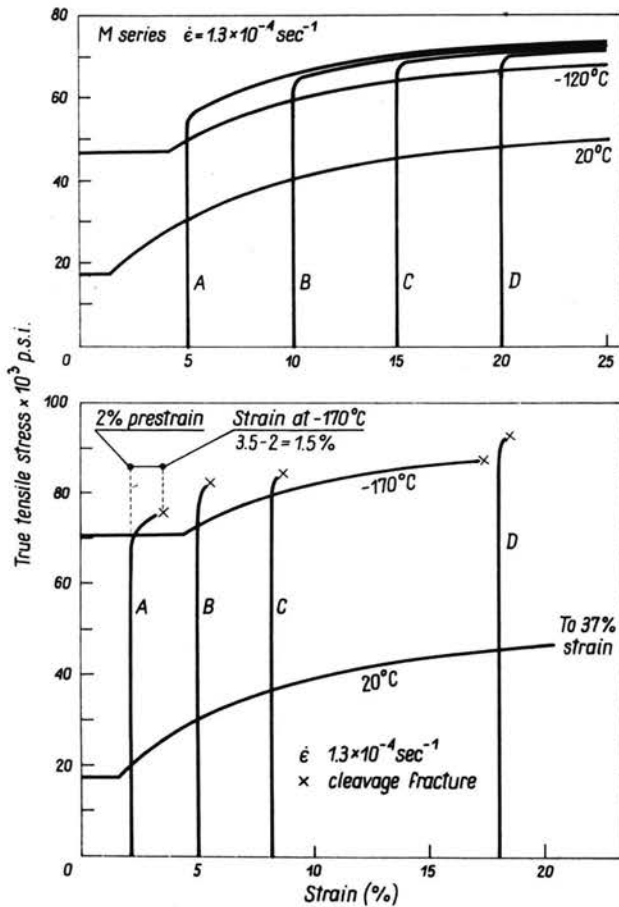


FIG. 18. The effect of prestrain at 293 K on the subsequent deformation of low carbon steel 0.05% C at 153 K (top) and 103 K (bottom); for all cases strain rate is the same $\dot{\epsilon} = 1.3 \times 10^{-4} \text{ s}^{-1}$, x — cleavage fracture; after [44].

results of interrupted temperature tests at 153 K show that the strain hardening rate is almost the same as for the entirely constant temperature test at 153 K, i.e. the complete set of stress-strain diagrams is almost parallel. This cannot be expected to hold generally in incremental strain rate experiments when $\dot{\gamma}_i < \dot{\gamma}_r$, mainly due to the fact that deformation in the first portion of such tests occurs isothermally, and in the second — adiabatic, whereas during exclusively dynamic deformation the process is entirely adiabatic. This effect should lead to the convergence of all dynamic stress-strain curves but not of quasi-static curves after dynamic prestraining. Such an effect was observed for low carbon steel (0.02% C) in [45] and is shown in Fig. 5. The estimate of thermal softening effects in the low temperature region (~ 100 K) shows that this is not the only factor causing strain rate history effects in steels [40, 41]. Other contributing factors involve the structural changes accompanying plastic deformation at a particular strain rate or temperature. For instance, at ambient temperatures and slow straining an additional hardening occurs associated with a dynamic strain ageing effect. However, it seems unlikely that such

a mechanism occurs at temperatures lower than room temperature where strain rate history effects are intensified. For example, temperature history effects persisted at 293 K when the prestrain was carried out not at the initial strain rate $1.3 \times 10^{-4} \text{ s}^{-1}$ but at a rate ten times higher, $\dot{\epsilon} = 1.3 \times 10^{-3} \text{ s}^{-1}$, [44].

Another possibility, suggested by microscopic observations [44], concentrates on microstructural changes during plastic deformation. It has been observed that for 0.05% C steel prior deformation at the ambient temperature inhibits general twinning on resumption of straining at low temperatures ($\sim 100 \text{ K}$). Thus, for a given initial strain at room temperature, a subsequent straining at low temperatures introduces a higher back stress resulting in a higher flow stress as compared to an entirely low temperature test. In addition, single-grain microcracks have been found after some plastic deformation at low temperatures. This was observed in specimens pre-strained at room temperature as well as strained entirely at a low temperature. Microcracks obviously can increase the athermal back stress level.

Finally, a third possibility lies in expected differences in dislocation multiplication rates at high and low strain rates or temperatures. The increased strain rate sensitivity at low temperatures and high strain rates may be attributed to the activation of more dislocation sources at higher strain rates with less activity (a smaller average displacement) per source than at lower rates. This effect leads to the conclusion that mobile dislocation density begins to be stress-dependent, and the strain rate increment is not only a function of dislocation velocity, which is stress dependent, but also a stress dependent function of the mobile dislocation density. Thus differentiation of the Orowan equation (1) (see for example [43]) leads to a more general result:

$$(1) \quad \dot{\gamma} = \chi \rho_m b \bar{V}(\tau, T),$$

$$(2) \quad d\dot{\gamma} = \chi b \left[\bar{V}(\tau, T) \left(\frac{\partial \rho_m}{\partial \tau} \right)_T d\tau + \rho_m(\tau, T) \left(\frac{\partial \bar{V}}{\partial \tau} \right)_T d\tau \right],$$

where \bar{V} is an average dislocation velocity, ρ_m is the density of mobile dislocations, and χ is an orientation factor, usually $\chi \approx 1$. At very high strain rates and low temperatures the dislocation velocity is relatively high and cannot accommodate itself to the imposed high stress. Consequently the first term in Eq. (2) should be dominating. In addition, in the high strain rate region, $\dot{\gamma} \approx 5 \times 10^3 \text{ s}^{-1}$, viscous resistance to dislocation motion becomes more important [20].

The idea that during high strain rate deformation at low temperatures more dislocation sources are generated serves to explain to some extent the result of interrupted tests for BCC metals shown schematically in Fig. 17, i.e. the straining history 4–5–6–7. In this case the flow stress after deformation at a high strain rate is lower than that obtained by straining entirely at the low strain rate, see Figs. 1, 2, 3 and 5. This implies that many dislocation sources already existing in the material due to the initial deformation at a high strain rate, for example as shown in [45], can be activated at a lower stress during additional straining at a low strain rate. This point of view is supported by the results of metallographic examinations reported in [27], which show that during loading at a strain rate of $\dot{\epsilon} \approx 5 \times 10^2 \text{ s}^{-1}$ deformation of medium carbon steel at room temperature occurs by fine slip, but that during slower straining at $\dot{\epsilon} \approx 10^{-3} \text{ s}^{-1}$ the slip bands are coarser.

Strain rate history effects observed within the dynamic strain ageing region result from the fact that the flow stress is governed not only by the strain rate but also by time itself. The explicit time dependence of flow stress is a manifestation of diffusion processes which interact with a moving dislocation [46]. Serrated yielding observed at lower strain rates in steels takes place when carbon or nitrogen atoms can diffuse fast enough to allow strain ageing to take place during plastic deformation. During this process an increased production of dislocations is observed [46]. Thus strain ageing should be dominant during slow deformation but will have limited influence during dynamic deformation, causing a substantial strain rate history effect, Figs. 15 and 16.

To conclude, strain rate history effects and perhaps temperature history effects dominate in the case of ferritic steels within two temperature regions: the low temperature domain ≤ 150 K, and the strain ageing temperature domain, $500 \text{ K} \pm 150 \text{ K}$. The physical nature of deformation history is different in each of these regions. The discovery of strain rate history effects at low temperatures is new and will require more attention in the future.

Acknowledgements

The authors gratefully acknowledge the support provided for this research by the National Science Foundation under grant MEA 79-23742 and through the Materials Research Laboratory at Brown University. The helpful suggestions of Mr. R. H. HAWLEY and the skillful typing of Debra FIRTH are gratefully acknowledged.

References

1. J. D. CAMPBELL, *Dynamic plasticity of metals*, J. Springer, 1972 (Lectures at International Centre for Mechanical Sciences, Udine, Italy, 1970).
2. U. S. LINDHOLM, *Techniques of metals research*, Ed. R. F. BUNSHAH, Vol. 5, Part 2, Interscience, New York 1971.
3. U. S. LINDHOLM, *Mechanical properties at high rate of strain*, Ed. J. HARDING, The Institute of Physics, Conf. Series No. 21, London-Bristol 1974.
4. J. DUFFY, *Mechanical properties at high rates of strain*, 1979, Ed. J. HARDING, The Institute of Physics, Conf. Series No. 47, Bristol-London 1979.
5. J. KLEPACZKO, *Arch. Mech.*, **24**, 187, 1972.
6. J. KLEPACZKO, *J. Mech. Phys. Solids*, **16**, 255, 1968.
7. P. S. SENSENY, J. DUFFY and R. H. HAWLEY, *J. Appl. Mech.*, **45**, 60, 1978.
8. A. M. ELEICHE and J. D. CAMPBELL, Technical Report AFML-TR-76-90, Air Force Material Laboratory, Ohio, March 1976.
9. J. KLEPACZKO, R. A. FRANTZ and J. DUFFY, *Rozpr. Inż.* **25**, 3, 1977.
10. R. A. FRANTZ and J. DUFFY, *J. Appl. Mech.*, **39**, 939, 1972.
11. C. W. MCGREGOR and J. C. FISHER, *J. App. Mech.*, **12**, A-217, 1945.
12. M. J. MANJOINE, *J. Appl. Mech.*, **11**, A-211, 1944.
13. A. NADAI and M. J. MANJOINE, *Proc. ASTM*, **40**, 822, 1940 (Part I).
14. A. NADAI and M. J. MANJOINE, *J. Appl. Mech.*, **8**, A-77, 1941 (Parts II and III).
15. J. M. KRAFFT, *Response of metals to high velocity deformation*, Interscience, 1961. Eds. P. G. SHEWMON and V. F. ZACKAY.
16. K. J. MARSH and J. D. CAMPBELL, *J. Mech. Phys. Solids*, **11**, 49, 1963.
17. D. L. DAVIDSON, U. S. LINDHOLM, and L. M. YEAKLEY, *Acta Met.*, **14**, 703, 1966.

18. J. KLEPACZKO, *Int. J. Solids and Struct.*, **5**, 533, 1969.
19. R. J. MACDONALD, R. L. CARLSON and W. T. LANKFORD, *Proc. ASTM*, **56**, 704, 1956.
20. J. D. CAMPBELL and W. G. FERGUSON, *Phil. Mag.*, **21**, 63, 1970.
21. N. NAGATA, S. YOSHIDA and Y. SOHIMO, *Trans. ISIY*, **10**, 173, 1970.
22. J. D. CAMPBELL and T. L. BRIGGS, *J. of Less-Common Metals*, **40**, 235, 1975.
23. U. F. KOCKS, A. S. ARGON and M. F. ASHBY, *Thermodynamics and kinetics of slip*, Pergamon Press, Oxford 1975.
24. E. J. RIPLING and G. SACHS, *Trans. AIME*, **185**, 78, 1949.
25. G. S. STONE and H. CONRAD, data published by H. CONRAD in: *High Strength Materials*, J. Wiley, N. Y. p. 440 1965.
26. T. NAKAMURA, S. SAKUI and Y. OHTAKARA, *Supplement Trans. JIM*, **9**, 905, 1968.
27. J. D. CAMPBELL and J. DUBY, *Proc. Conf. on Properties of Materials at High Rates of Strain*, Inst. of Mech. Engrs., London 1957.
28. J. D. CAMPBELL and C. J. MAIDEN, *J. Mech. Phys. Solids*, **6**, 53, 1957.
29. R. C. SMITH, *Exp. Mech.*, **1**, 153, 1961.
30. J. HARDING, Discussion of paper by Klepaczko and Duffy in *Proc. Conf. on Mechanical Properties at High Rates of Strain*, The Inst. of Phys., Conf. Ser. No. 21, 191, London 1974.
31. T. NICHOLAS, *Exp. Mech.*, **11**, 370, 1971.
32. J. KLEPACZKO, *Foundations of plasticity*, Ed. A. SAWCZUK, Nordhoff, 1973.
33. E. KREMPL, *J. Mech. Phys. Solids*, **27**, 363, 1979.
34. J. DUFFY, *Mechanical properties at high rates of strain*, Ed. J. HARDING, The Inst. of Phys., Conf. Ser. No. 21, London 1974.
35. J. KLEPACZKO, Technical Report, Division of Engineering, Brown University, 1974.
36. R. A. FRANTZ and J. DUFFY, *J. Appl. Mech.*, 939, December 1972.
37. J. D. CAMPBELL, A. M. ELEICHE and M. C. C. TSAO, *Fundamental aspects of structural alloy design*, Ed. R. I. JAFFEE and B. A. WILCOX, Plenum Press, New York 1977.
38. M. L. WILSON, R. H. HAWLEY and J. DUFFY, Technical Report, Division of Engineering, Brown University, NSF-18532/8, 1979.
39. J. DUFFY and R. H. HAWLEY, Technical Report, Division of Engineering, Brown University, 1981 (in preparation).
40. J. KLEPACZKO and J. DUFFY, *Mechanical testing for deformation model development*, Ed. R. D. ROHDE and J. C. SWEARENGEN, ASTM STP No. 720, American Society for Testing and Materials, Philadelphia 1981.
41. J. KLEPACZKO, *The relation of thermally activated flow in BCC metals and ferritic steels to strain rate history and temperature-history effects*, Technical Report, Brown University DMR-79-23257/2, Providence 1981.
42. J. KLEPACZKO, *Materials Science and Engineering*, **18**, 121, 1975.
43. A. R. CHAUDHURI, J. R. PATEL and L. G. RUBIN, *J. Appl. Phys.* **33**, 2736, 1962.
44. T. C. LINDLEY, *Acta Met.*, **13**, 681, 1965.
45. K. TANAKA, T. NOJIMA and H. ISHIKAWA, *Proc. 15th Japan Congr. on Materials Res.*, The Soc. of Materials Research, 1972.
46. A. S. KEH, Y. NAKADA and W. C. LESLIE, *Dislocation dynamics*, Eds. A. R. ROSENFELD *et. al.*, McGraw-Hill, New York 1968.

POLISH ACADEMY OF SCIENCES
INSTITUTE OF FUNDAMENTAL TECHNOLOGICAL RESEARCH
and

DIVISION OF ENGINEERING
BROWN UNIVERSITY, PROVIDENCE, USA.

Received September 2, 1981.